CIRP Annals - Manufacturing Technology 67 (2018) 571–574

Contents lists available at ScienceDirect

CIRP Annals - Manufacturing Technology

journal homepage: http://ees.elsevier.com/cirp/default.asp

Fabrication of un-coated transparent superhydrophobic sapphire surface using laser surface ablation and heat treatment

Chi-Vinh Ngo [a,b,c], Doo-Man Chun (2) [a,*]

[a] School of Mechanical Engineering, University of Ulsan, Republic of Korea
[b] Changchun Institute of Optics, Fine Mechanics and Physics, Chinese Academy of Sciences, Changchun, China
[c] The Institute of Optics, University of Rochester, Rochester, NY, USA

ARTICLE INFO

Article history:
Available online 3 May 2018

Keywords:
Laser beam machining (LBM)
Surface modification
Transparent superhydrophobic sapphire

ABSTRACT

Sapphire is a widely used hard transparent material for optics and protective windows, and a superhydrophobic coating on sapphire can prevent contamination by self-cleaning. However, the coating can be easily degraded according to time and heat. In this research, transparent superhydrophobic sapphire surfaces were fabricated via laser surface ablation, without coating, for good stability and heat resistance. The laser ablated surface showed hydrophilic initially, but the wettability transition to superhydrophobic was achieved after an additional simple heat treatment. Contact angle and transmittance were measured to confirm the superhydrophobicity and transparency, and surface analysis was performed to explain the wetting mechanism.

1. Introduction

In recent decades, superhydrophobic surfaces, which are surfaces with water droplet contact angles (CAs) greater than 150° and sliding angles (SAs) smaller than 10°, have attracted great attention both in academia and in industry due to their unique characteristics, such as water repellence and self-cleaning. These unique characteristics of superhydrophobic surfaces are formed by low surface energies and unique structures, such as nano-micro hierarchical structures or micro unitary structures, on a surface. Superhydrophobic surfaces have been fabricated on a variety of polymer, metal, silicon, and ceramic substrates by using various processes, including chemical vapor deposition (CVD), silanization, laser beam machining, molding, and photolithography [1–5].

Among these materials, ceramic materials have good thermal stability and chemical inertness, and superhydrophobic surfaces on ceramic substrates have been heavily investigated owing to their application in self-cleaning, anti-fogging, and capturing of harmful CO_2 or volatile organic compounds. Coatings or chemical treatments have been widely utilized to realize super-hydrophobicity on ceramics [6–10]. Unfortunately, current chemical coating techniques are harmful to the environment and ineffective over extended periods of time; the processes utilize toxic chemicals and the coating layers can be easily degraded as a function of time and heat, especially at high temperatures [11]. The limitations of the current research prohibit widespread manufacturing of superhydrophobic ceramic surfaces.

To produce a superhydrophobic ceramic surface, a laser beam machining has been developed; this is advantageous due to its reproducibility, precision, and relatively low surface contamination [12,13]. Jagdheesh used picosecond laser ablation on Al_2O_3 and stored the ablated substrate in air for three days to progress the wetting state of Al_2O_3 from hydrophilic to nearly superhydrophobic/superhydrophobic [14]. However, it is difficult to take advantage of the performance of this surface for self-cleaning applications. Other researchers have used laser beam machining, but they have used additional chemical coating to improve the performance of superhydrophobic surfaces in real applications [15,16].

Recently, in our previous research, we proposed a simple and environmentally friendly technique that uses laser beam ablation and heat treatment to manipulate metals and metal alloys [17–19]. Here, in this research, transparent superhydrophobic sapphire was developed by using the same laser surface ablation and heat treatment technique. In addition to pure metals and metal alloys, this technique was demonstrated to be applicable to ceramic materials, which play an important role in many engineering fields and real applications. Additionally, the initial transparency of the sapphire was maintained after laser beam ablation by controlling laser power and laser beam path. The effects of the laser power and laser beam path on the superhydrophobicity and transparency were investigated. Moreover, the mechanism was explained by utilizing various surface characteristic techniques, such as scanning electron microscopy (SEM), 3D confocal microscopy, energy-dispersive X-ray spectroscopy (EDS), X-ray diffraction (XRD), and Fourier transform infrared spectroscopy (FTIR). The transparent superhydrophobic sapphire showed good performance in terms of its superhydrophobicity and transparency. Furthermore, the stability of superhydrophobic surface was evaluated after 15 days in the ambient air and over 10 times cycles of heat treatment.

2. Experiment

2.1. Fabrication of transparent superhydrophobic sapphire

A Q-switched Nd:YAG 355 nm UV nanosecond pulse laser system was set up, as shown in Fig. 1. A laser source provided the

* Corresponding author.
E-mail address: dmchun@ulsan.ac.kr (D.-M. Chun).

https://doi.org/10.1016/j.cirp.2018.04.085
0007-8506/

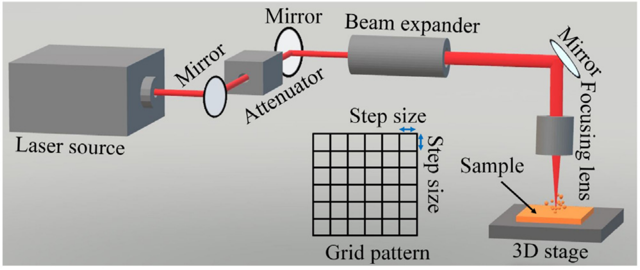

Fig. 1. Laser surface ablation system and pattern design.

Table 1
Fabrication parameters of laser surface ablation.

Name of parameter	Value
Power (W)	0.1; 0.25; 0.5; 0.75; 1; 1.5; 2
Pulse frequency (Hz)	20
Pulse duration (ns)	20
Stage speed (mm/s)	1
Step size or pitch (μm)	100
Number of samples	Six for each power

laser beam and mirrors were used to orient the beam. The attenuator controlled the laser beam power, while a beam expander was used to increase the laser beam diameter. The laser beam was converged by a focusing lens to ablate on the substrate, which was placed on a 3-axis translation stage. A grid pattern design as the laser beam path with different step sizes or pitches was used in this research; this design shows isotropic wetting in all observation directions [20,21].

A 0.43-mm-thick sapphire wafer (Al_2O_3 C-Plane, 4science, Korea) was used to investigate the effect of the laser power on the superhydrophobicity and transparency. The fabrication parameters are summarized in Table 1. After laser ablation, the surfaces of laser-machined samples with different selected laser powers were observed as shown in Fig. 2. The confocal images show a clear grid pattern design. When the laser beam ablated the surface, lots of small debris was formed. The debris was concentrated significantly along the fabricated path to form micro-burr structures, while less debris was found on the flat areas between the fabricated paths. When the laser power was increased, the micro burr heights also increased. The average values, which were measured 10 times for each sample via confocal microscopy, were 0.85, 2.07, 3.00, 3.04, 4.01, 5.60, and 6.95 μm for laser powers of 0.1, 0.25, 0.5, 0.75, 1, 1.5, and 2 W, respectively. When the laser power increased from 0.25 W, the laser ablation induced debris covered almost the entire flat area between the fabricated paths. However, when the laser power was reduced to 0.1 W, the power was not strong enough and clear, flat, square-shaped areas with a brighter color appeared (in Fig. 2a). These areas appear to include the flat bare sapphire substrate and a small quantity of debris. The formation of the micro burr structure and debris may affect the wetting state and transparency of the sapphire surface. After laser surface ablation, all samples were put in a commercial oven for six hours at 200 °C. The samples were then removed and cooled at room temperature to investigate their wettability and transmittance.

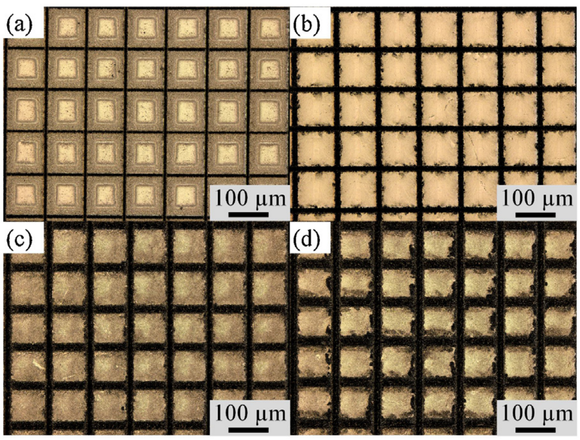

Fig. 2. Confocal microscope images of laser-ablated surfaces with different laser powers: (a) 0.1 W, (b) 0.25 W, (c) 1 W, and (d) 2 W.

2.2. Effect of laser power on wettability

The wettability of samples was evaluated with 10-μL water droplets with a contact angle meter (SmartDrop, FemtoFab, Korea). The unprocessed flat sapphire wafer showed hydrophilic character (83°). After laser ablation, sapphire substrates treated with different laser powers showed increased hydrophilicity, with CAs smaller than 40° and no SAs, as shown in Fig. 3. The error bars represent the maximum and minimum values. However, after heat treatment, all samples became superhydrophobic. Samples treated with laser powers greater than 0.1 W showed high CAs (>170°) and small SAs (<10°), which are good for self-cleaning applications. Samples treated with 0.1 W had CAs of approximately 160°, which are smaller than the other samples. Additionally, these 0.1 W-treated samples had no SAs. The water droplet might be contacting the flat, square areas (with brighter colors in Fig. 2a), which included the flat bare sapphire and very small quantities of the debris. The flat sapphire between fabricated paths was hydrophilic and strongly attracted water droplets. Therefore, the water droplet could not roll off the surface and no SA was observed.

Superhydrophobic sapphire samples treated with different laser powers were stored in ambient air after heat treatment. The wettability (CA, SA) was evaluated again after 15 days to investigate the stability of the superhydrophobicity. All samples maintained their superhydrophobicity and typical CA images are shown in Fig. 4. The sample treated at 0.25 W showed hydrophilic character after laser ablation but became superhydrophobic after heat treatment; it maintained this property for well over 15 days. Fig. 4d shows the SAs of samples treated at 0.25 W (4°) with a tilting speed of 0.8°/s.

As shown in Fig. 5, the contact angle hysteresis (CAH) was measured using the captive bubble method to confirm the performance of superhydrophobicity. All samples showed small

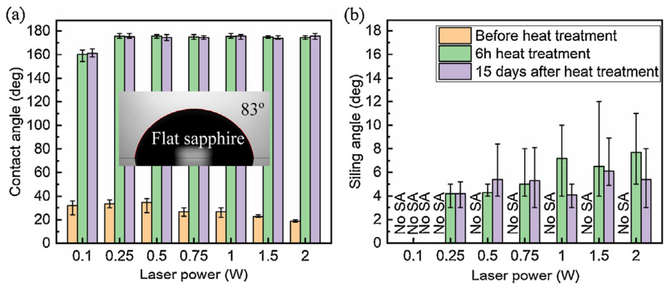

Fig. 3. (a) Contact angles and (b) sliding angles of sapphire treated with different laser powers before heat treatment, after heat treatment, and after being stored in air for 15 days after the heat treatment.

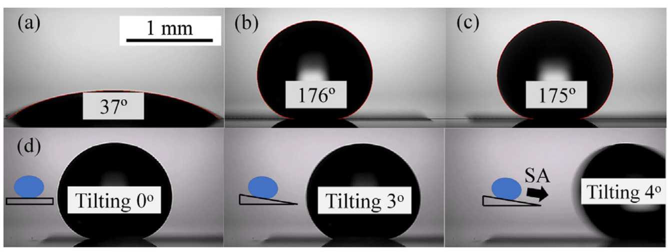

Fig. 4. Water droplet images on the 0.25 W laser-ablated sample: (a) just after laser ablation, (b) after heat treatment, (c) after being stored in air for 15 days after heat treatment, and (d) sliding angle after heat treatment.

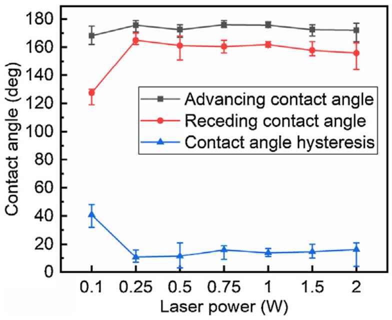

Fig. 5. Contact angle hysteresis of sapphire treated with different laser powers.

CAH (from approximately 10° to less than 20°), except for samples treated at 0.1 W. Among the investigated laser power values, samples treated with 0.25 W showed the best superhydrophobicity.

2.3. Effect of laser power on transparency

The transmittance values of the surfaces treated with different laser powers were measured with a UV–vis-NIR spectro-photometer in the visible spectrum range from 380 nm to 750 nm, as shown in Fig. 6. When the laser power increased, the transmittance of the sapphire decreased because of the increased burr formation. Among them, the samples treated at 0.25 W, which had the best superhydrophobicity, showed a small average transmittance drop (approximately less than 10%) relative to the unprocessed smooth sapphire and less than 1% deviation in transmittance on five different samples.

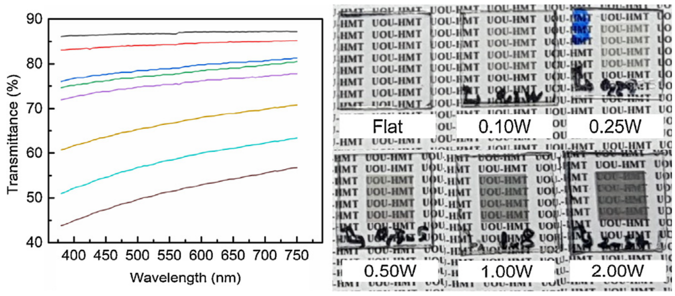

Fig. 6. Transmittance results of unprocessed flat sapphire and laser-ablated sapphire with different laser powers (from top to bottom curve: unprocessed, 0.1, 0.25, 0.5, 0.75, 1, 1.5 and 2 W).

3. Discussion

3.1. Mechanism

The mechanism of superhydrophobicity was explained by investigating the nano-micro hierarchical structures and low surface energy. After laser ablation, clear micro burr structures were formed along the fabricated paths (in Figs. 2 and 7). Additionally, nanostructures were also created on the flat areas between the fabricated paths; however, these structures were not observed on the unprocessed smooth sapphire. Therefore, nano-micro hierarchical structures were produced after laser surface ablation. However, the appearance of nano-micro structures was not enough to make the sapphire to become superhydrophobic; after laser ablation, all samples were still hydrophilic. It is clear that another factor contributed to this mechanism.

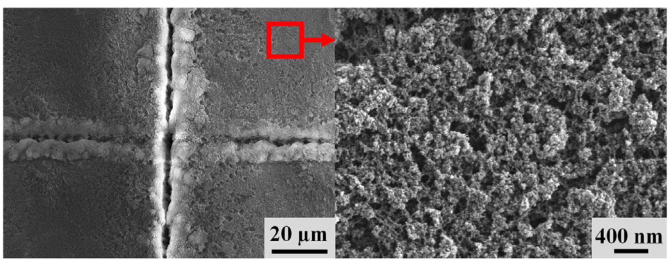

Fig. 7. FESEM images of laser-induced debris nanostructures on flat areas between the fabricated paths on 0.25 W-treated sample.

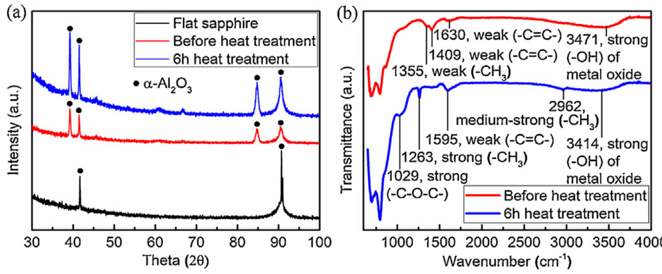

Fig. 8. (a) XRD and (b) FTIR results of laser-ablated sapphire samples.

After heat treatment, all samples became superhydrophobic. The crystalline structures before and after heat treatment did not change, as shown in Fig. 8a . However, a change in the surface chemistry was found on the micro-burrs and nanostructures, as shown in Table 2. The amount of carbon content on the structures after heat treatment increased, especially on the micro burrs. The carbon content comes from organic adsorption, as shown in Fig. 8b. After laser ablation, the –OH group of Al_2O_3 can adsorb organic matter from ambient air, leading to the appearance of several weak hydrophobic groups (–CH_3). Under heat treatment, this organic adsorption was accelerated, causing the appearance of strong hydrophobic groups (–CH_3) (low surface energy). Therefore, the nano-micro structures, with their adsorbed strongly hydrophobic bonding, caused sapphire to become superhydrophobic. The organic adsorption has been found on the laser-ablated aluminum where aluminum oxide appeared after laser beam ablation [19].

Table 2
EDS results.

Element	Before heat treatment		After heat treatment	
	At burr	Flat areas between fabricated paths	At burr	Flat areas between fabricated paths
C	9.0	7.8	15.8	8.6
O	66.2	67.5	64.9	69.7
Al	24.7	24.8	18.6	21.5

3.2. Heat resistance

Three superhydrophobic sapphire samples treated with a laser power of 0.25 W were prepared to evaluate the heat resistance properties. After heat treatment for six hours at 200 °C, samples were stored in air for three days; this constitutes one cycle. This cycle was repeated over 10 times, as shown in Fig. 9. All samples maintained their superhydrophobicity for long heat treatments at a high temperature (200 °C).

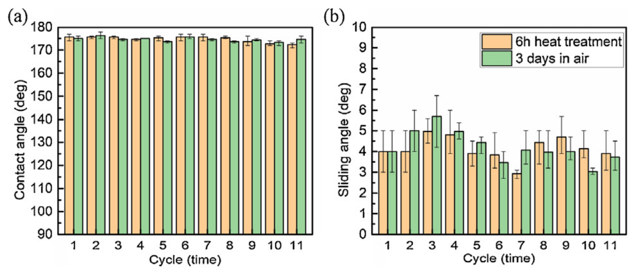

Fig. 9. Heat resistance of superhydrophobic sapphire.

3.3. Effect of step size

The step sizes of sapphire samples treated with a laser power of 0.25 W were changed from 50 to 300 µm. All samples with

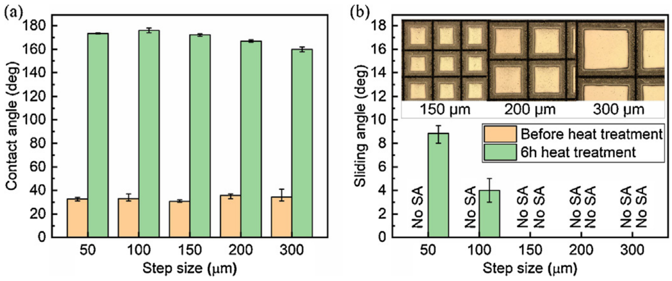

Fig. 10. (a) Contact angles and (b) sliding angles of sapphire treated with different step sizes before heat treatment and after heat treatment.

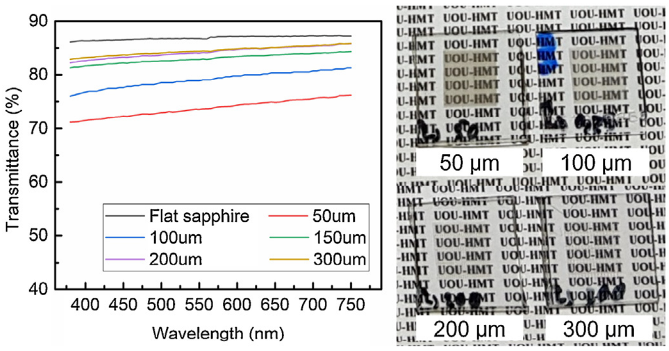

Fig. 11. Transmittance results of laser-ablated sapphire with different step sizes.

different step sizes showed high CAs (>160°), but only the samples with step sizes smaller than 150 µm showed small SAs (<10°) as shown in Fig. 10. The samples with step sizes of 150, 200, and 300 µm showed hydrophilic flat areas with no debris (brighter color areas in the inset of Fig. 10(b)). When the step size increased, the transmittance of the sapphire increased because of the reduction of fabricated area as shown in Fig. 11. To fabricate a transparent superhydrophobic ceramic material, using a laser power of 0.25 W with a 100 µm step size is a good method.

3.4. Potential applications

In this study, the transmittance of surface is reduced when reducing the step size or increasing the laser power. Additionally, among fabrication parameters, samples showed the best superhydrophobic performance at 100 µm step size with 0.25 W. The performance of superhydrophobic sapphire is shown in Fig. 12. Samples showed low adhesion and the bouncing effect with respect to water droplets. This demonstrates their high-quality superhydrophobicity. Additionally, samples also showed the self-cleaning effect with the tilting angle of 4°. The obtained surfaces can be used for self-cleaning, low-adhesion applications.

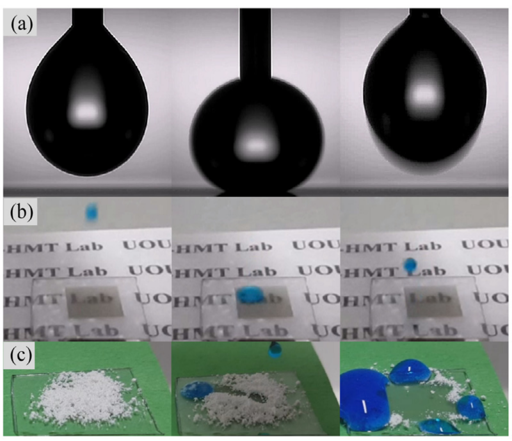

Fig. 12. Performance of superhydrophobic sapphire: (a) water adhesion, (b) bouncing effect, and (c) self-cleaning effect.

4. Conclusion

A transparent superhydrophobic ceramic can be produced by a simple and environmentally friendly technique by using a combination of laser surface ablation and heat treatment. Best our knowledge, the transparent superhydrophobic ceramic has been firstly fabricated on sapphire only with laser ablation and heat treatment, without any chemical coatings. Laser-ablated sapphire samples showed good superhydrophobicity (CA > 170°, SA < 7°) and high transmittance over 75% in visible light. Additionally, the surfaces were stable and demonstrated heat resistance under high-temperature conditions. The mechanism was also explained in terms of the laser-induced nano-micro structures and surface chemistry (organic absorption). Several potential uses, such as self-cleaning optics, protective windows, and low water adhesion applications, were proposed.

Acknowledgment

This research was supported by a National Research Foundation of Korea (NRF) grant (NRF-2018R1A2B6004012).

References

[1] Vilar R (2016) *Laser Surface Modification of Biomaterials: Techniques and Applications*, Woodhead Publishing.
[2] Cohen N, Dotan A, Dodiuk H, Kenig S (2016) Superhydrophobic Coatings and Their Durability. *Materials and Manufacturing Processes* 31(9):1143–1155.
[3] Wang S, Liu K, Yao X, Jiang L (2015) Bioinspired Surfaces with Superwettability: New Insight on Theory, Design, and Applications. *Chemical Reviews* 115:8230–8293.
[4] Ngo C-V, Chun D-M (2016) Laser Printing of Superhydrophobic Patterns from Mixtures of Hydrophobic Silica Nanoparticles and Toner Powder. *Scientific Reports* 6:36735.
[5] Tran V-HT, Lee B-K (2017) Novel Fabrication of a Robust Superhydrophobic PU@ZnO@Fe_3O_4@SA Sponge and Its Application in Oil-water Separations. *Scientific Reports* 7:17520.
[6] Shang Q, Zhou Y (2016) Fabrication of Transparent Superhydrophobic Porous Silica Coating for Self-cleaning and Anti-fogging. *Ceramics International* 42:8706–8712.
[7] Yu X, An L, Yang J, Tu S-T, Yan J (2015) CO_2 Capture Using a Superhydrophobic Ceramic Membrane Contactor. *Journal of Membrane Science* 496:1–12.
[8] Kujawa J, Al-Gharabli S, Kujawski W, Knozowska K (2017) Molecular Grafting of Fluorinated and Nonfluorinated Alkylsiloxanes on Various Ceramic Membrane Surfaces for the Removal of Volatile Organic Compounds Applying Vacuum Membrane Distillation. *ACS Applied Materials & Interfaces* 9(7):6571–6590.
[9] Abdulhameed MA, Othman MHD, Ismail AF, Matsuura T, Harun Z, Rahman MA, Puteh MH, Jaafar J, Rezaei M, Hubadillah SK (2017) Carbon Dioxide Capture Using a Superhydrophobic Ceramic Hollow Fibre Membrane for Gas-liquid Contacting Process. *Journal of Cleaner Production* 140:1731–1738.
[10] Kujawa J, Cerneaux S, Kujawski W (2015) Highly Hydrophobic Ceramic Membranes Applied to the Removal of Volatile Organic Compounds in Pervaporation. *Chemical Engineering Journal* 260:43–54.
[11] Parkin IP, Palgrave RG (2005) Self-cleaning Coatings. *Journal of Materials Chemistry* 15(17):1689–1695.
[12] Meijer J (2004) Laser Beam Machining (LBM), State of the Art and New Opportunities. *Journal of Materials Processing Technology* 149(1):2–17.
[13] Meijer J, Du K, Gillner A, Hoffmann D, Kovalenko VS, Masuzawa T, Ostendorf A, Poprawe R, Schulz W (2002) Laser Machining by Short and Ultrashort Pulses, State of the Art and New Opportunities in the Age of the Photons. *CIRP Annals — Manufacturing Technology* 51(2):531–550.
[14] Jagdheesh R (2014) Fabrication of a Superhydrophobic Al_2O_3 Surface Using Picosecond Laser Pulses. *Langmuir* 30(40):12067–12073.
[15] Boinovich LB, Domantovskiy AG, Emelyanenko AM, Pashinin AS, Ionin AA, Kudryashov SI, Saltuganov PN (2014) Femtosecond Laser Treatment for the Design of Electro-insulating Superhydrophobic Coatings with Enhanced Wear Resistance on Glass. *ACS Applied Materials & Interfaces* 6(3):2080–2085.
[16] Stroj S, Kasemann S, Domke M, Piredda G, Zehetner J, Matylitskaya V (2017) Transparent Superhydrophobic Surfaces with High Adhesion Generated by the Combination of Femtosecond Laser Structuring and Wet Oxidation. *Applied Surface Science* 420:550–557.
[17] Chun D-M, Ngo C-V, Lee K-M (2016) Fast Fabrication of Superhydrophobic Metallic Surface Using Nanosecond Laser Texturing and Low-temperature Annealing. *CIRP Annals — Manufacturing Technology* 65(1):519–522.
[18] Ngo C-V, Chun D-M (2017) Fast Wettability Transition from Hydrophilic to Superhydrophobic Laser-textured Stainless Steel Surfaces under Low-temperature Annealing. *Applied Surface Science* 409:232–240.
[19] Ngo C-V, Chun D-M (2018) Control of Laser-ablated Aluminum Surface Wettability to Superhydrophobic or Superhydrophilic Through Simple Heat Treatment or Water Boiling Post-processing. *Applied Surface Science* 435:974–982.
[20] Chun D-M, Davaasuren G, Ngo C-V, Kim C-S, Lee G-Y, Ahn S-H (2014) Fabrication of Transparent Superhydrophobic Surface on Thermoplastic Polymer Using Laser Beam Machining and Compression Molding for Mass Production. *CIRP Annals — Manufacturing Technology* 63(1):525–528.
[21] Davaasuren G, Ngo C-V, Oh H-S, Chun D-M (2014) Geometric Study of Transparent Superhydrophobic Surfaces of Molded and Grid Patterned Polydimethylsiloxane (PDMS). *Applied Surface Science* 314:530–536.